The Journal of Arthroplasty

Definition of Femoral Morphotypes Based on the Coronal Plane Alignment of the Hip Classification

--Manuscript Draft--

Manuscript Number:	JOA-D-25-03103R1
Article Type:	Original Article
Corresponding Author:	Ricarda Stauss, Dr. Carl von Ossietzky University Oldenburg, School of Medicine and Health Sciences, Division of Orthopaedics at Campus Pius-Hospital, Oldenburg, Germany GERMANY
First Author:	Ricarda Stauss, Dr.
Order of Authors:	Ricarda Stauss, Dr.
	Peter Savov, Dr.
	Florian Biestmann
	Mike Brueggemann
	Michael A. Mont, Dr.
	Thorsten M. Seyler, Dr.
	Max Ettinger, Prof. Dr.
Manuscript Region of Origin:	Europe
Abstract:	Background: In total hip arthroplasty (THA), accurate reconstruction of physiological joint biomechanics is determined by the individual patient's proximal femoral anatomy and stem design. Previous studies demonstrated a wide variation of femoral canal shapes and an association with extramedullary geometrical features. The purpose of this study was to propose a comprehensive classification for the coronal plane alignment of the hip (CPAH) that incorporates intramedullary and extramedullary parameters. We sought to determine the distribution of femoral morphotypes in an osteoarthritic cohort and to assess the reconstructive potential of four common femoral stem designs in each CPAH type. Methods: The preoperative radiographs of 2,345 patients undergoing primary uncemented THA were retrospectively analyzed, including Dorr classification, neck-shaft angle (NSA), femoral offset (FO), and femoral offset ratio (FOR). The CPAH classification defines nine morphotypes based on the combination of Dorr type and NSA. Each morphotype is categorized into a normal- and a high-offset subgroup. Digital templating was conducted to assess the reconstruction of FO, leg-length (LL), and the agreement between anatomy and stem geometry. Results: CPAH types 2N, 5N, 5H, 6N, and 8N accounted for a combined percentage of 82% (n = 1,928), whereas the remaining morphotypes represented less common anatomical constitutions. Canal shape, FO, and NSA were associated with demographic characteristics (age, $P < 0.001$; sex, $P < 0.001$). Subgroup analyses stratified by CPAH types revealed that the reconstructive potential of each stem design depends on the patient's femoral morphotype. Across all CPAH types, the short stem was the best-fit implant, whereas a mismatch between anatomy and stem design was evident in up to 80% of the cases using the anatomic stem design. Conclusions: CPAH classification provides a comprehensive classification system for femoral morphotypes. It enables a phenotyping approach in THA planning and provides practical guidance for individualized implant selection.

Definition of Femoral Morphotypes Based on the Coronal Plane Alignment of the Hip Classification

Ricarda Stauss [1], Peter Savov [1], Florian Biestmann [1,2], Mike Brueggemann [2], Michael A. Mont [3], Thorsten M. Seyler [4], Max Ettinger [1]

[1] Carl von Ossietzky University Oldenburg, School of Medicine and Health Sciences, Division of Orthopaedics at Campus Pius-Hospital, Oldenburg, Germany

[2] Hannover Medical School, Department of Orthopaedic Surgery, Hannover, Germany

[3] The Rubin Institute for Advanced Orthopedics, Lifebridge Health, Sinai Hospital of Baltimore, Baltimore, MD, USA

[4] Department of Orthopaedic Surgery, Duke University, Durham, North Carolina, USA

Abstract

Background: In total hip arthroplasty (THA), accurate reconstruction of physiological joint biomechanics is determined by the individual patient's proximal femoral anatomy and stem design. Previous studies demonstrated a wide variation of femoral canal shapes and an association with extramedullary geometrical features. The purpose of this study was to propose a comprehensive classification for the coronal plane alignment of the hip (CPAH) that incorporates intramedullary and extramedullary parameters. We sought to determine the distribution of femoral morphotypes in an osteoarthritic cohort and to assess the reconstructive potential of four common femoral stem designs in each CPAH type.

Methods: The preoperative radiographs of 2,345 patients undergoing primary uncemented THA were retrospectively analyzed, including Dorr classification, neck-shaft angle (NSA), femoral offset (FO), and femoral offset ratio (FOR). The CPAH classification defines nine morphotypes based on the combination of Dorr type and NSA. Each morphotype is categorized into a normal- and a high-offset subgroup. Digital templating was conducted to assess the reconstruction of FO, leg-length (LL), and the agreement between anatomy and stem geometry.

Results: CPAH types 2N, 5N, 5H, 6N, and 8N accounted for a combined percentage of 82% (n = 1,928), whereas the remaining morphotypes represented less common anatomical constitutions. Canal shape, FO, and NSA were associated with demographic characteristics (age, $P < 0.001$; sex, $P < 0.001$). Subgroup analyses stratified by CPAH types revealed that the reconstructive potential of each stem design depends on the patient's femoral morphotype. Across all CPAH types, the short stem was the best-fit implant, whereas a mismatch between anatomy and stem design was evident in up to 80% of the cases using the anatomic stem design.

Conclusions:

CPAH classification provides a comprehensive classification system for femoral morphotypes. It enables a phenotyping approach in THA planning and provides practical guidance for individualized implant selection.

Keywords: CPAH classification, coronal plane alignment of the hip, femoral morphotype, Dorr classification, total hip arthroplasty, stem design, individualized arthroplasty

Introduction

In total hip arthroplasty (THA), the accurate reconstruction of physiological joint biomechanics is crucial for the postoperative outcome and is determined by the patient's proximal femoral anatomy and the design of the prosthesis. The Dorr classification defines three distinct femoral canal shapes based on intramedullary parameters [1]. However, previous studies identified a much higher variability of intramedullary shapes and extramedullary geometrical parameters that are relevant for the reconstruction of physiological joint biomechanics by THA [2-4]. Active shape modeling and subsequent cluster analyses identified a minimum of ten distinct patterns of femoral canal shape, each characterized by distinct geometrical measures including femoral offset (FO) and neck-shaft angle (NSA) [3]. These findings indicate an association between canal shape and joint geometry that has not yet been incorporated in a classification system. In THA, inaccurate reconstruction of these parameters is associated with adverse functional outcomes, wear of bearing surfaces, and reduced implant survival rates [5-9]. Consequently, implant selection is one of the most important decisions in preoperative THA planning to achieve the best possible agreement between hip anatomy and implant geometry. In primary THA, femoral components can be classified into six categories based on implant geometry, modularity, and length; each associated with with distinct biomechanical characteristics in terms of fixation principles and load transfer [10,11]. Although implant choice and fixation type are often determined by the patient's age and bone quality, there remains uncertainty about which stem design allows for the best possible reconstruction of the individual patient's anatomic constitution. Therefore, a novel classification of femoral morphotypes that has the capacity to determine which stem design provides the best reconstructive potential for the individual anatomy would be of value.

The purpose of this study was to propose a classification system for the coronal plane alignment of the hip (CPAH) that combines intramedullary and extramedullary geometric parameters. We sought to determine the distribution of femoral morphotypes in a large osteoarthritic patient collective and to assess the reconstructive potential of common femoral stem designs in each CPAH type.

Methods

CPAH classification

In this single-center, retrospective study, patients who underwent primary, cementless THA between 2016 and 2021 were screened for eligibility. After applying exclusion criteria, 2,345 radiographs were analyzed (Figure 1).

Radiological analysis was performed using preoperative, low-centered anteroposterior radiographs, which were obtained using a standardized protocol [12]. Patients were positioned supine, and legs were internally rotated by 15 degrees using a leg retainer. To ensure a reproducible radiographic projection, quality criteria included symmetric obturator foramina, neutral pelvic positioning, and symmetric visualization of the lesser trochanters. Severe deformities of the acetabulum and proximal femur precluding reliable determination of the femoral head and hip center of rotation were excluded (Figure 1).

Measurements followed a standardized algorithm (Figure 2) and were performed using Carestream Picture Archiving and Communication System software (Carestream Health Inc., Rochester, New York, USA). Intra- and interobserver reliabilities for radiological measurements were calculated for 20 randomly selected radiographs using intraclass correlation coefficients (ICC) with a two-way random effects model for absolute agreement and revealed excellent intra- and interobserver ICCs (respective ranges: 0.991 to 0.998 and 0.911 to 0.998). Dorr classification was assessed using the cortical index (CI) (Dorr A > 0.6, Dorr B 0.5 – 0.6, Dorr C <0.5) [1,13]. The NSA was measured as the angle between the femoral neck axis and femoral shaft axis (coxa vara < 120°, coxa valga > 140°). The FO was measured as the perpendicular distance between the center of the femoral head and the femoral shaft axis. Femoral offset ratio (FOR) was defined as the ratio of FO divided by the cortical width 10 cm distal to the lesser trochanter. By normalizing the absolute value of FO to the femoral shaft diameter, the FOR allows the identification of anatomic subtypes with an increased offset relative to femoral size.

The CPAH classification was conceptualized as a hierarchical framework integrating intramedullary and extramedullary parameters of proximal femoral anatomy in the coronal plane. In the classification matrix, Dorr types are set against the NSA subgroups, defining nine distinct femoral morphotypes (Figure 3). FOR was incorporated as a secondary stratification parameter within each morphotype to account for proportional variation in femoral offset relative to femoral size. Each morphotype is further categorized into a normal (FOR_N) and high offset (FOR_H) cohort. The cut-off value for the FOR_H subtypes was defined using a distribution-based approach and set at 1.60 (mean FOR plus one standard deviation). This threshold was selected to identify anatomic subtypes with a clearly increased FOR, representing clinically relevant high-offset configurations within each CPAH type.

Patients' mean age was 66 years (range, 16 to 92), and 60.2% were women. Dorr types A, B, and C accounted for 31.3, 55.2, and 13.5%, respectively. Mean NSA was 130.3° (range, 105 to 162°), and mean FO was 46.3 mm (range, 11.6 to 76.1). Overall, 80.6% of the cases were classified as coxa norma, 8.1% as coxa vara, and 11.3% as coxa valga. The mean FOR was 1.40 (SD 0.2), and 15.8% were categorized as high-offset subtypes (FOR_H).

Digital templating study

For each CPAH type, five cases were randomly selected using a simple random sampling approach in Statistical Package for the Social Sciences (SPSS) Statistics software. Representative femoral components were selected based on their use in the recent national and international arthroplasty registry reports [14,15], and stem geometry was categorized using the classification proposed by Radaelli et al. [11]: straight stem (Type A, n = 3 stem designs), shortened quadrangular taper stem (Type B3, n = 1 stem design), anatomic fit-and-fill (Type C2, n = 1 stem design), or short-stem prostheses (Type F, n = 2 stem designs) (Figure 1).

Digital templating was conducted using mediCAD® 2D software V7.0 (Hectec GmbH, Altdorf/Landshut, Germany) following the standardized protocol for calibration and the definition of anatomical landmarks. For acetabular cup placement, inclination was set at 40 to 45°, and the native center of rotation was restored to avoid alterations of the acetabular offset and compensatory changes of the femoral and global offset. Planning of the femoral component was followed the respective manufacturer's instructions, aiming for the reconstruction of the native FO, leg-length equalization, and an adequate meta- and diaphyseal anchorage as appropriate per stem design. For each implant type, the stem option that enabled the best possible reconstruction of FO and leg length was selected, including available lateralized stem options. Modular head options were limited to standard and medium lengths to avoid offset compensation through excessive head lengthening.

Outcome parameters for part II of the study were FO reconstruction (ΔFO planned – preoperative) and leg-length equalization, assessed as leg-length discrepancy (LLD, affected minus contralateral hip). THA reconstruction was considered adequate when the following criteria were met: (1) ΔFO within zero to five mm [7], (2) LLD $\leq$ 10 mm, and (3) agreement between proximal femoral anatomy and implant geometry, defined as an adequate meta-/diaphyseal anchorage or canal fill as appropriate per stem design and no mismatch between canal shape and stem design [16].

Data analyses

Scatterplots were created to display the distribution of CPAH types. Normal distribution was tested using the Shapiro–Wilk tests. *Chi*–square tests were used to compare categorical data. Group differences were calculated using Student's *t*-tests or Mann–Whitney *U*-tests. We used one-way Analysis of Variance (ANOVA) and Kruskal–Wallis tests for multiple-group comparisons. Bonferroni adjustments were applied for multiple testings (α = 0.05). Statistical analyses were performed using SPSS Statistics 29 (IBM Corporation, Armonk, New York, USA). Statistical significance was set at $P < 0.05$. Figures were created using GraphPad Prism 10.6.0 (GraphPad Inc., La Jolla, California, USA). The study was approved by the local ethics committee (#10232_BO_K_2022).

Results

CPAH classification of femoral morphotypes

The CPAH classification matrix defines nine femoral morphotypes by the combination of Dorr type and NSA and 18 subtypes stratified by FOR (Table 1, Figures 3 and 4). In this Caucasian study cohort, the most common morphotypes were CPAH 2N, 5N, 5H, 6N, and 8N, accounting for a combined percentage of 82% of the cases. The proportion of FOR_H subtypes was highest in varus hips, whereas the combination of valgus NSA and FOR_H was not observed in the entire cohort.

Demographic characteristics differed significantly between the CPAH types (Table 2). An inverse correlation was observed between age and both canal shape and NSA. The mean age was lowest in patients who have Dorr A femora, whereas Dorr C was associated with higher age (64 versus 69 years, r = -0.134, $P < 0.001$), and the mean age was lowest in patients categorized as coxa valga (mean age: 63 years versus 69 years in coxa valga versus coxa vara, r = -0.186, $P < 0.001$). A positive correlation was observed between age and FO (r = 0.199, $P < 0.001$) and FOR_H ($P < 0.001$). Women were associated with lower CI values ($P < 0.001$) and higher NSA ($P < 0.001$). The FOR_H was associated with higher age ($P < 0.001$) and women ($P = 0.012$).

Digital templating – Hip Coronal Reconstruction

In the varus CPAH types 1, 4, and 7, the best FO reconstruction was achieved in the quadrangular taper and short-stem subgroups, resulting in a combined percentage of 93.3 to 98.3% of adequate FO reconstructions within zero to five mm (Figure 5A and Table 3) ($P < 0.001$). Templating of the straight stem was associated with a reduction of FO, reflected by a combined percentage of 40.0% of adequate FO reconstructions in all varus CPAH types combined ($P < 0.001$). The best leg-length reconstruction was achieved using the B3 stem,

whereas the highest LLD was observed in the anatomic stem cohort (P = 0.004) (Figure 5B). For varus hips, the best agreement between femoral anatomy and stem design was achieved with the short-stem designs, while templating revealed a mismatch between anatomy and implant design in 25.5% of the straight stem and 40.0% of the anatomic stem simulations (P < 0.001).

In the high-offset morphotypes, the most anatomic FO reconstruction was achieved in the quadrangular taper and short-stem subgroups (P < 0.001). In contrast, templating of the straight stem components was associated with an offset reduction. The planned LLD did not differ significantly between the groups (P = 0.111).

In the valgus subtypes CPAH 3, 6, and 9, mean ΔFO was increased with all stem designs (Figure 5A and Table 3). In all valgus morphotypes combined, the best FO reconstruction was achieved with the short stem, whereas the anatomic stem was associated with the highest increase (P < 0.001). In valgus hips, the best reconstruction was achieved using the short stem and B3 stem, whereas the straight and anatomic stems could not be simulated due to a mismatch between femoral anatomy and implant geometry in 57.8 and 66.7% of the cases, respectively (P < 0.001).

In CPAH types 1 to 3, characterized by Dorr A anatomy, the short stem and B3 stem prostheses matched the femoral canal shape in 100.0 and 84.0% of the cases (P < 0.001). In CPAH types 7 to 9 with Dorr C anatomy, the best agreement was observed for the short stem and B3 stem, whereas templating revealed a mismatch between canal shape and implant design in 32.0% of the straight stem and 64.0% of the anatomic stem simulations (P < 0.001). Detailed results of the digital templating study stratified by CPAH types and stem design are provided in Figures 5 A to B, Table 3, and Supplemental Tables S1A to B.

Discussion

In this study, we introduce the CPAH classification that defines nine distinct femoral morphotypes combining intramedullary and extramedullary geometrical parameters that are crucial for the reconstruction of hip biomechanics in THA. The most important findings of our study were that the variability of proximal femoral anatomy is oversimplified by the existing classification systems and that a *one-size-fits-all* concept using a single femoral stem design does not have the reconstructive potential to achieve an anatomic reconstruction across the distinct femoral morphotypes.

CPAH classification of femoral morphotypes

Our results demonstrated a substantial variability of proximal femoral anatomy and an association with demographic characteristics in a large patient collective. In the present study,

NSA ranged from 105 to 162°, and FO ranged from 11.6 to 76.1 mm. Although the mean values are consistent with evidence from previously published studies [17-19], the overall range detected in this cohort indicates a much greater variability of femoral anatomy. In addition, our results complement the evidence for an association between canal shape an demographical characteristics by revealing not only sex-specific differences in proximal femoral anatomy, but also an association between age and both NSA and canal shape [1,2,20,21]. Although a sex-specific approach has been discussed for THA before [22], the considerable inter-individual variability in femoral anatomy underscores the need for a more individualized approach. The CPAH classification provides a pragmatic and comprehensive system for the definition of femoral morphotypes and has the potential to contribute to a phenotyping approach in THA. Despite most cases being attributable to CPAH types 2, 5, and 8, the classification matrix further defines less common femoral morphotypes that may present challenges for the reconstruction of hip geometry in THA. Although no high-offset subgroup was observed in the valgus CPAH types 3, 6, and 9, these theoretical subtypes were included for completeness, as an inadequate reconstruction of FO in primary THA is associated with the risk of consecutive phenotype changes.

Digital templating – Hip Coronal Reconstruction

Subgroup analyses stratified by CPAH type and stem design revealed considerable group differences for the agreement between implant geometry and proximal femoral anatomy indicating that the reconstructive potential of each stem design depends on the individual femoral morphotype.

In primary THA, an accurate reconstruction of hip geometry and joint biomechanics is crucial for the clinical and functional outcome [6,7,9,23,24]. A recent study by Vorimore et al. revealed a substantial impact of the reconstruction of FO and LL on the clinical outcome, and the best results were observed in cases with a coronal reconstruction within a 2.5 mm range [6]. Therefore, a thorough analysis of femoral anatomy and optimal implant selection are crucial to optimize coronal hip reconstruction. To our knowledge, no study has yet compared the reconstructive potential of different stem geometries following a phenotyping approach.

In the varus and high offset CPAH types, the most anatomic reconstruction of FO and LL, and the highest proportions of adequate THA reconstructions were achieved with the short stem and B3 stem designs. In calcar-guided short-stem THA, stem position is determined by the osteotomy level, which enhances the capacity to accurately restore FO across different femoral morphotypes [25]. In varus and FOR_H phenotypes, a high osteotomy and consecutive varus position of the stem enable the reconstruction of high FO anatomies, whereas a deep resection allows for an anatomic FO reconstruction in valgus morphotypes. The B3 stem design also follows the medial calcar and is characterized by a reduced distal geometry, which minimizes

proximal-distal mismatch between stem design and canal shape and increases the reconstructive potential across various femoral morphotypes [11, 26]. In contrast, our results demonstrate a lower reconstructive potential of the straight and anatomic stem designs, especially in CPAH types characterized by high femoral offset, extensive varus or valgus NSA, as well as Dorr A or C canal shapes. These stem designs achieve diaphyseal anchorage, which potentially limits coronal hip reconstruction in cases with outlier configurations of the constitutional NSA and canal shape. In most conventional stem designs, neck length increases with stem size, which results in an increased offset and leg lengthening [26]. However, this linear relationship between canal shape and neck length does not reflect the variability of proximal femoral anatomy. Moreover, the reconstruction of high-offset anatomies using lateralized stems and large femoral head lengths is associated with inferior outcomes and an increased risk for aseptic loosening [27].

In the entire cohort, the short stem was the best-fit implant. In CPAH types 2N, 4N, 4H, 5N, and 5H, sufficient fixation was achieved in 80 to 100% with all four stem geometries. For the straight stem, a mismatch between proximal femoral anatomy and stem geometry was observed in 26% of the varus and 58% of the valgus morphotypes, as well as 36% of Dorr A and 32% of Dorr C anatomies. The anatomic stem demonstrated a mismatch with consecutive insufficient fixation in 40% of the varus and 67% of the valgus CPAH types, as well as 28% of Dorr A and 64% of Dorr C morphotypes. In accordance with our results, Boese et al. reported a poor agreement between femoral anatomy and implant geometry of a straight stem design in 30% of the cases [16]. In their study, the poor reconstruction was predominantly observed in cases with a high FO, the combination of low FO and low femoral neck height, and valgus hips. Ishii et al. also found an association between femoral canal shape and a proximal-distal mismatch for straight stem designs [28]. These findings consistently demonstrate that a single implant design does not have the reconstructive potential to achieve an anatomic reconstruction across all distinct femoral morphotypes. The CPAH classification draws on the concept of a phenotyping approach, which has been successfully introduced in total knee arthroplasty by the Coronal Plane Alignment of the Knee (CPAK) classification, which provides a pragmatic framework linking knee phenotypes to alignment strategies [29]. Similarly, the CPAH classification defines distinct femoral morphotypes based on a combination of intramedullary and extramedullary parameters and links these to the reconstructive potential of established stem designs. While the four stem categories evaluated in this study represent the most commonly used implant geometries in current clinical practice, the CPAH classification enables a structured, anatomy-based assessment that allows the identification of patients in whom a mismatch between stem design and proximal femoral anatomy is anticipated. Accordingly, preoperative CPAH assessment has the potential to guide surgeons

toward a more individualized implant selection and to identify cases in which a broader implant portfolio may be necessary to achieve an adequate reconstruction of hip biomechanics.
Current evidence on the reconstructive potential of stem geometries is limited, as the majority of studies investigate specific implant types, which restricts the transferability of the results. In this context, CPAH classification provides not only a pragmatic framework for the assessment of proximal femoral anatomy and coronal reconstruction in THA but also enables consistent reporting in future research.

Potential limitations

The current study should be interpreted considering its potential limitations. Although a standardized radiological imaging protocol was followed, conventional radiographs remain susceptible to projection-related inaccuracies potentially affecting quantitative measurements. The study focuses exclusively on the two-dimensional assessment of proximal femoral anatomy in the coronal plane and sagittal femoral geometry was not assessed in this study. The anterior femoral curvature varies considerably between individuals and may influence diaphyseal fit, particularly for longer stem designs that achieve distal fixation [30]. The degree of anterior bowing is directly associated with posterior stem tilting [30], and femoral anteversion has been shown to be independent of the coronal morphotype [31], suggesting that sagittal and transversal parameters represent distinct anatomical dimensions warranting complementary classification. Additionally, femoral anteversion and anterior femoral offset correlate with femoral rotation and sagittal hip biomechanics [32,33]. While computed tomography-based analyses could provide a multidimensional assessment of proximal femoral anatomy, anteroposterior radiographs constitute the standard preoperative imaging modality. Therefore, CPAH classification can easily be incorporated into clinical practice. Future research, including statistical shape modelling of three-dimensional imaging data, may allow for a multi-planar expansion of the classification to address sagittal stem alignment, femoral torsion and restoration of anterior femoral offset. In our study, femoral anatomy was investigated in an osteoarthritic Caucasian cohort; hence, the distributions of CPAH types may differ in other populations. Furthermore, the clinical applicability of CPAH classification is limited in cases with proximal femoral deformities which potentially compromise the reliable determination of anatomical landmarks. THA reconstruction was simulated in a digital templating study, enabling for a highly standardized assessment of the reconstructive potential of different stem designs in the coronal plane. By the anatomic restoration of the hip center of rotation, the biomechanical effects of cup positioning were excluded. Although previous studies demonstrated high accuracy and reliability for digital templating, the transferability to postoperative THA reconstruction may be limited. The retrospective study design and the templating approach precluded the assessment of functional outcomes. Future prospective

studies are warranted to verify our results and to examine the effects on postoperative radiological and functional outcomes.

Conclusions

In conclusion, the novel CPAH classification is a comprehensive classification system that defines nine distinct femoral morphotypes based on intramedullary and extramedullary geometrical parameters. Our results demonstrate that the reconstructive potential of femoral stem designs depends on the patient's individual proximal femoral anatomy. Therefore, CPAH enables a phenotyping approach in preoperative THA planning and provides practical guidance for implant choice.

References

1. **Dorr LD, Faugere MC, Mackel AM, Gruen TA, Bognar B, Malluche HH.** Structural and cellular assessment of bone quality of proximal femur. Bone. 1993;14(3):231-42. doi: 10.1016/8756-3282(93)90146-2

2. **Noble PC, Alexander JW, Lindahl LJ, Yew DT, Granberry WM, Tullos HS.** The anatomic basis of femoral component design. Clin Orthop Relat Res. 1988;(235)(235):148-65.

3. **Merle C, Waldstein W, Gregory JS, Goodyear SR, Aspden RM, Aldinger PR, et al.** How many different types of femora are there in primary hip osteoarthritis? An active shape modeling study. Journal of Orthopaedic Research: Official Publication of the Orthopaedic Research Society. 2014;32(3):413-22. doi: 10.1002/jor.22518

4. **Carmona M, Tzioupis C, LiArno S, Faizan A, Argenson JN, Ollivier M.** Upper Femur Anatomy Depends on Age and Gender: A Three-Dimensional Computed Tomography Comparative Bone Morphometric Analysis of 628 Healthy Patients' Hips. J Arthroplasty. 2019;34(10):2487-93. doi: 10.1016/j.arth.2019.05.036

5. **McGrory BJ, Morrey BF, Cahalan TD, An KN, Cabanela ME.** Effect of Femoral Offset on Range of Motion and Abductor Muscle Strength after Total Hip Arthroplasty. J Bone Joint Surg Br. 1995;77(6):865-9.

6. **Vorimore C, Innmann M, Mavromatis S, Speirs A, Verhaegen JCF, Merle C, et al.** Impact of Offset and Leg Length on Functional Outcomes Post-Total Hip Arthroplasty: How Accurate Should Coronal Reconstruction Be? J Arthroplasty. 2024;39(9s2):S332-S9.e2. doi: 10.1016/j.arth.2024.06.017

7. **Cassidy KA, Noticewala MS, Macaulay W, Lee JH, Geller JA.** Effect of femoral offset on pain and function after total hip arthroplasty. J Arthroplasty. 2012;27(10):1863-9. doi: doi.org/10.1016/j.arth.2012.05.001

8. **Charles MN, Bourne RB, Davey JR, Greenwald AS, Morrey BF, Rorabeck CH.** Soft-tissue balancing of the hip: the role of femoral offset restoration. Instructional course lectures. 2005;54:131-41.

9. **Innmann MM, Spier K, Streit MR, Aldinger PR, Bruckner T, Gotterbarm T, et al.** Comparative Analysis of the Reconstruction of Individual Hip Anatomy Using 3 Different Cementless Stem Designs in Patients With Primary Hip Osteoarthritis. J Arthroplasty. 2018;33(4):1126-32. doi: 10.1016/j.arth.2017.11.026

10. **Kheir MM, Drayer NJ, Chen AF.** An Update on Cementless Femoral Fixation in Total Hip Arthroplasty. J Bone Joint Surg Am. 2020;102(18):1646-61. doi: 10.2106/JBJS.19.01397

11. **Radaelli M, Buchalter DB, Mont MA, Schwarzkopf R, Hepinstall MS.** A New Classification System for Cementless Femoral Stems in Total Hip Arthroplasty. J Arthroplasty. 2022. doi: 10.1016/j.arth.2022.09.014

12. **Clohisy JC, Carlisle JC, Beaulé PE, Kim YJ, Trousdale RT, Sierra RJ, et al.** A systematic approach to the plain radiographic evaluation of the young adult hip. J Bone Joint Surg Am. 2008;90 Suppl 4(Suppl 4):47-66. doi: 10.2106/JBJS.H.00756

13. **Lim YW, Huddleston JI, Goodman SB, Maloney WJ, Amanatullah DF.** Proximal Femoral Shape Changes the Risk of a Leg Length Discrepancy After Primary Total Hip Arthroplasty. J Arthroplasty. 2018;33(12):3699-703. doi: 10.1016/j.arth.2018.08.008

14. **German Arthroplasty Registry (Endoprothesenregister Deutschland - EPRD)**: Annual Report 2024. https://www.eprd.de/ fileadmin/user_upload/Dateien/Publikationen/ Berichte/Jahresbericht2024-Status5_2024-10-22_F.pdf [20.12.24].

15. **American Joint Replacement Registry (AJRR)**: 2024 Annual Report. Rosemont, IL: American Academy of Orthopaedic Surgeons (AAOS), 2024. https://www.aaos.org/ globalassets/registries/12.18.24_highlights-from-the-ajrr-2024-annual-report.pdf [20.12.24].

16. **Boese CK, Dargel J, Jostmeier J, Eysel P, Frink M, Lechler P.** Agreement Between Proximal Femoral Geometry and Component Design in Total Hip Arthroplasty: Implications for Implant Choice. J Arthroplasty. 2016;31(8):1842-8. doi: 10.1016/j.arth.2016.02.015

17. **Boese CK, Dargel J, Oppermann J, Eysel P, Scheyerer MJ, Bredow J, et al.** The femoral neck-shaft angle on plain radiographs: a systematic review. Skeletal Radiol. 2016;45(1):19-28. doi: 10.1007/s00256-015-2236-z

18. **Toogood PA, Skalak A, Cooperman DR.** Proximal femoral anatomy in the normal human population. Clin Orthop Relat Res. 2009;467(4):876-85. doi: 10.1007/s11999-008-0473-3

19. **Müller M, Abdel MP, Wassilew GI, Duda G, Perka C.** Do post-operative changes of neck-shaft angle and femoral component anteversion have an effect on clinical outcome following uncemented total hip arthroplasty? Bone Joint J. 2015;97-b(12):1615-22. doi: 0301-620X.97B12.34654

20. **Karayiannis PN, Cassidy RS, Hill JC, Dorr LD, Beverland DE.** The Relationship Between Canal Diameter and the Dorr Classification. J Arthroplasty. 2020;35(11):3204-7. doi: 10.1016/j.arth.2020.05.066

21. **Casper DS, Kim GK, Parvizi J, Freeman TA.** Morphology of the proximal femur differs widely with age and sex: relevance to design and selection of femoral prostheses. J Orthop Res. 2012;30(7):1162-6. doi: 10.1002/jor.22052

22. **Traina F, De Clerico M, Biondi F, Pilla F, Tassinari E, Toni A.** Sex differences in hip morphology: is stem modularity effective for total hip replacement? J Bone Joint Surg Am. 2009;91 Suppl 6:121-8. doi: 10.2106/JBJS.I.00533

23. **Kayani B, Konan S, Thakrar RR, Huq SS, Haddad FS.** Assuring the long-term total joint arthroplasty: a triad of variables. Bone Joint J. 2019;101-B(1_Supple_A):11-8. doi: 10.1302/0301-620X.101B1.BJJ-2018-0377.R1

24. **Innmann MM, Maier MW, Streit MR, Grammatopoulos G, Bruckner T, Gotterbarm T, et al.** Additive Influence of Hip Offset and Leg Length Reconstruction on Postoperative Improvement in Clinical Outcome After Total Hip Arthroplasty. J Arthroplasty. 2018;33(1):156-61. doi: 10.1016/j.arth.2017.08.007

25. **Kutzner KP.** Same same but different: Introduction of a classification system in calcar-guided short-stem total hip arthroplasty. Hip Int. 2025;35(1):54-61. doi: 10.1177/11207000241286259

26. **Fink B, Morgan M, Schuster P.** Reconstruction of the anatomy of the hip in total hip arthroplasty with two different kinds of stems. BMC Musculoskelet Disord. 2022;23(1):212.

27. **Jud L, Rüedi N, Dimitriou D, Hoch A, Zingg PO.** High femoral offset as a risk factor for aseptic femoral component loosening in cementless primary total hip arthroplasty. Int Orthop. 2024;48(5):1217-24. doi: 10.1186/s12891-022-05152-9

28. **Ishii S, Homma Y, Baba T, Ozaki Y, Matsumoto M, Kaneko K.** Does the Canal Fill Ratio and Femoral Morphology of Asian Females Influence Early Radiographic Outcomes of Total Hip Arthroplasty With an Uncemented Proximally Coated, Tapered-Wedge Stem? J Arthroplasty. 2016;31(7):1524-8. doi: 10.1016/j.arth.2016.01.016

29. **MacDessi SJ, Griffiths-Jones W, Harris IA, Bellemans J, Chen DB.** Coronal Plane Alignment of the Knee (CPAK) classification. The Bone Joint J. 2021;103-B(2):329-37. doi: 10.1302/0301-620X.108B1.BJJ-2025-00062

30. **Noor EA, Dilogo IH, Silitonga J, Ramadhani R.** Analysis on association between sagittal stem alignment and early functional and radiological outcome following primary cementless total hip replacement. Eur J Orthop Surg Traumatol. 2024;34(4):2129-36. doi: 10.1007/s00590-024-03904-y

31. **Sariali E, Boukhelifa S.** Unlike Acetabular Anteversion, Femoral Anteversion Is Not Associated with the Hip Coronal Morphotype: An Anatomic Basis for a New Hip Morphotype Classification at Total Hip Arthroplasty. J Bone Joint Surg Am. 2025;107(12):1333-41. doi: 10.2106/JBJS.24.00489

32. **Dennis DA, Bryman JA, Smith GH, Pierrepont JW, Jennings JM, Rajpura A, et al.** How Do Changes in Femoral Anteversion Impact Femoral Rotation and Anterior Offset After Total Hip Arthroplasty? J Arthroplasty. 2025;40(1):152-9.e1. doi: 10.1016/j.arth.2024.07.027

33. **Dennis DA, Plaskos C, Pierrepont JW, O'Sullivan MD, Jennings JM, Smith GH.** Accuracy of Joint Center Reconstruction in Total Hip Arthroplasty and Its Effect on Postoperative Femoral Axial Rotation. J Arthroplasty. 2025;40(8s1):S152-S8.e3. doi: 10.1016/j.arth.2025.03.065.

Figures

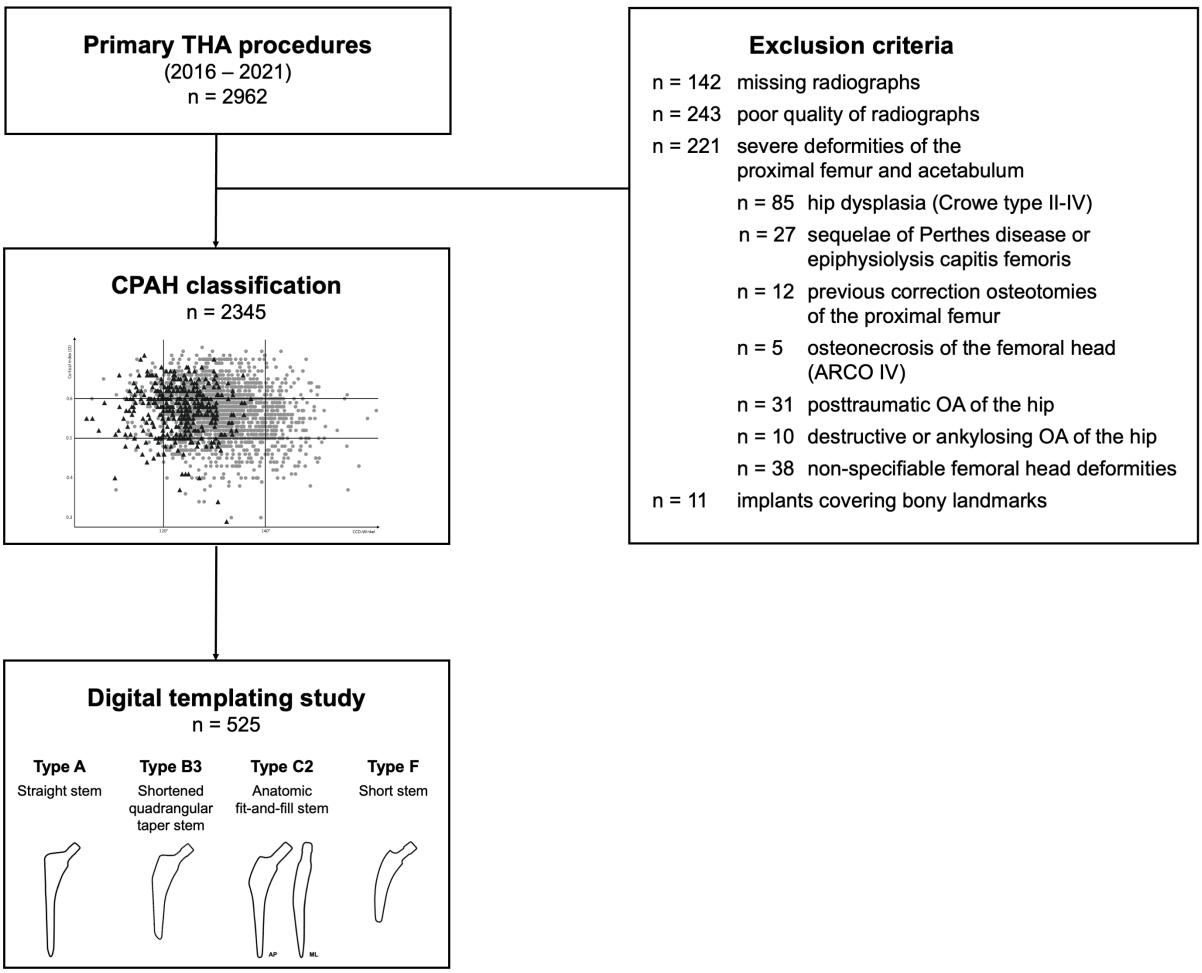

Figure 1 Flowchart of the study design.

ARCO, Association Research Circulation Osseous Classification; CPAH, Coronal Plane Alignment of the Hip Classification; OA, osteoarthritis; THA, total hip arthroplasty.

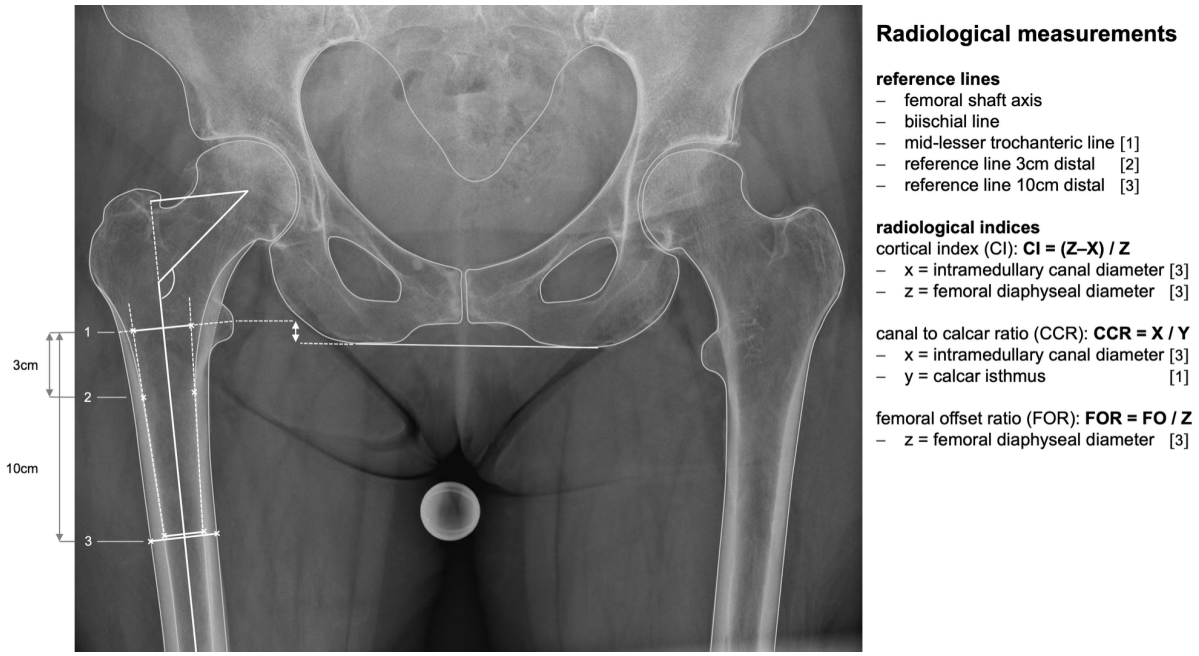

Figure 2 This figure shows the radiological measurements of femoral offset (FO), neck-shaft angle (NSA), and the radiological indices, including the Dorr classification and femoral offset ratio (FOR) in a preoperative low-centered antero-posterior radiograph of the pelvis.

	Coxa vara		Coxa norma		Coxa valga	
	FOR_N	FOR_H	FOR_N	FOR_H	FOR_N	FOR_H
Dorr A	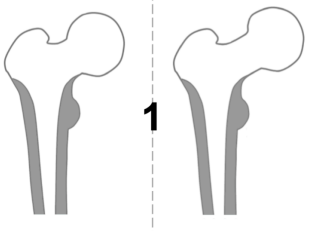 1		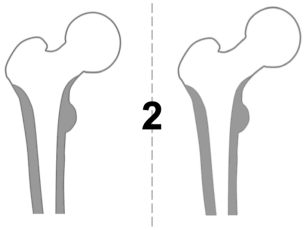 2		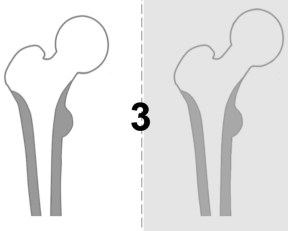 3	
Dorr B	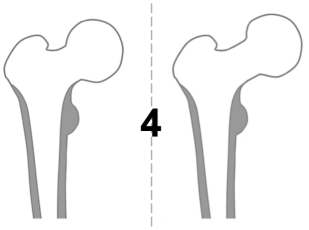 4		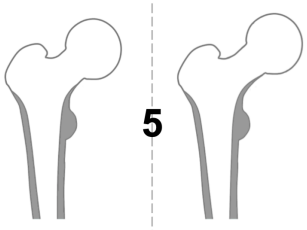 5		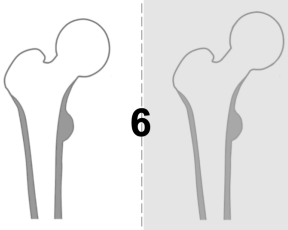 6	
Dorr C	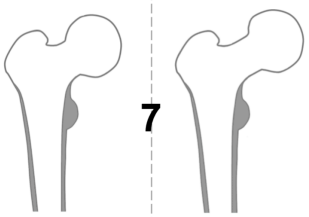 7		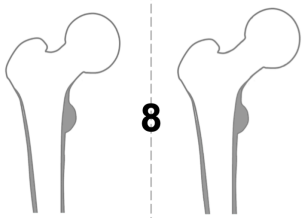 8		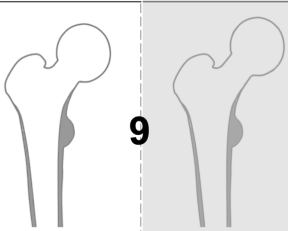 9	

Figure 3 The Coronal Plane Alignment of the Hip (CPAH) classification matrix defines nine femoral morphotypes by the combination of Dorr types and NSA subgroups. Each CPAH type is further subdivided into a normal (FOR_N) and a high offset subgroup (FOR_H).

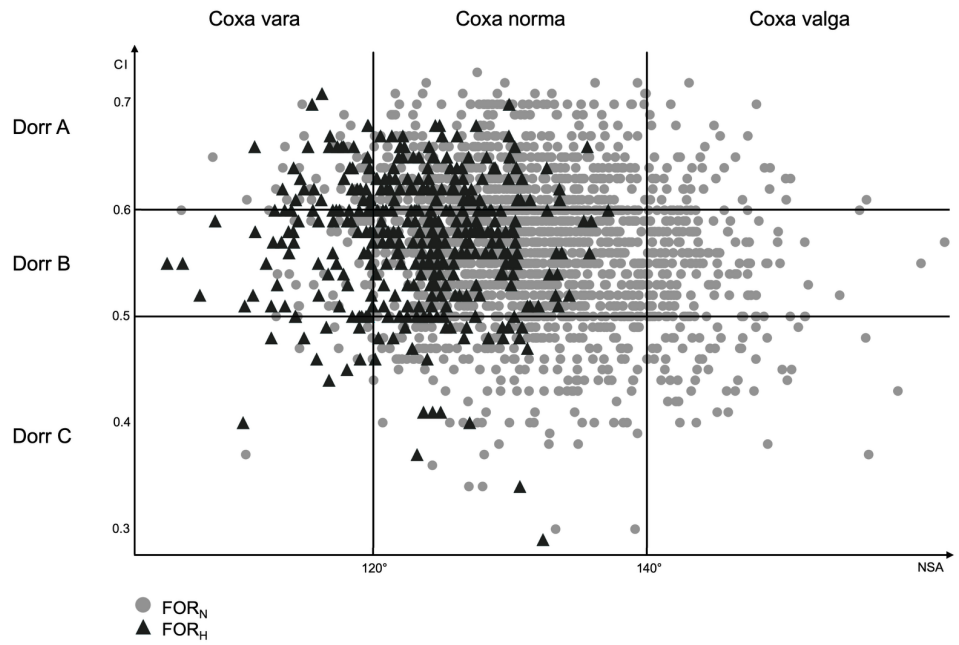

Figure 4: Scatterplot depicting the distribution of CPAH types. Dorr types are set against the subgroups by neck-shaft angle. The high-offset subgroup (FOR_H) is color-coded and represented by triangles.

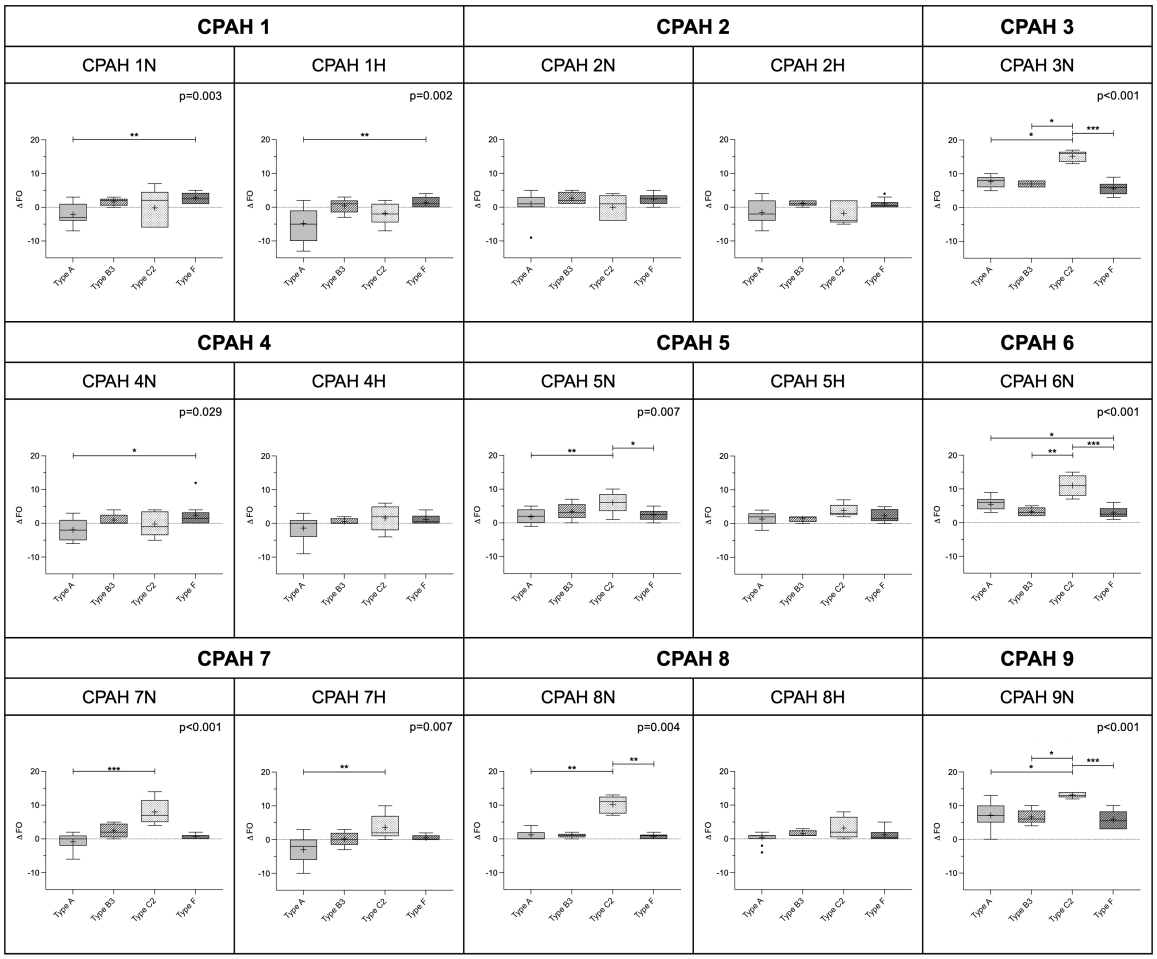
CPAH 1
CPAH 1N
CPAH 1H
p=0.003
p=0.002
CPAH 2
CPAH 2N
CPAH 2H
CPAH 3
CPAH 3N
p<0.001
CPAH 4
CPAH 4N
CPAH 4H
p=0.029
CPAH 5
CPAH 5N
CPAH 5H
p=0.007
CPAH 6
CPAH 6N
p<0.001
CPAH 7
CPAH 7N
CPAH 7H
p<0.001
p=0.007
CPAH 8
CPAH 8N
CPAH 8H
p=0.004
CPAH 9
CPAH 9N
p<0.001
Δ FO
Type A
Type B3
Type C2
Type F

A

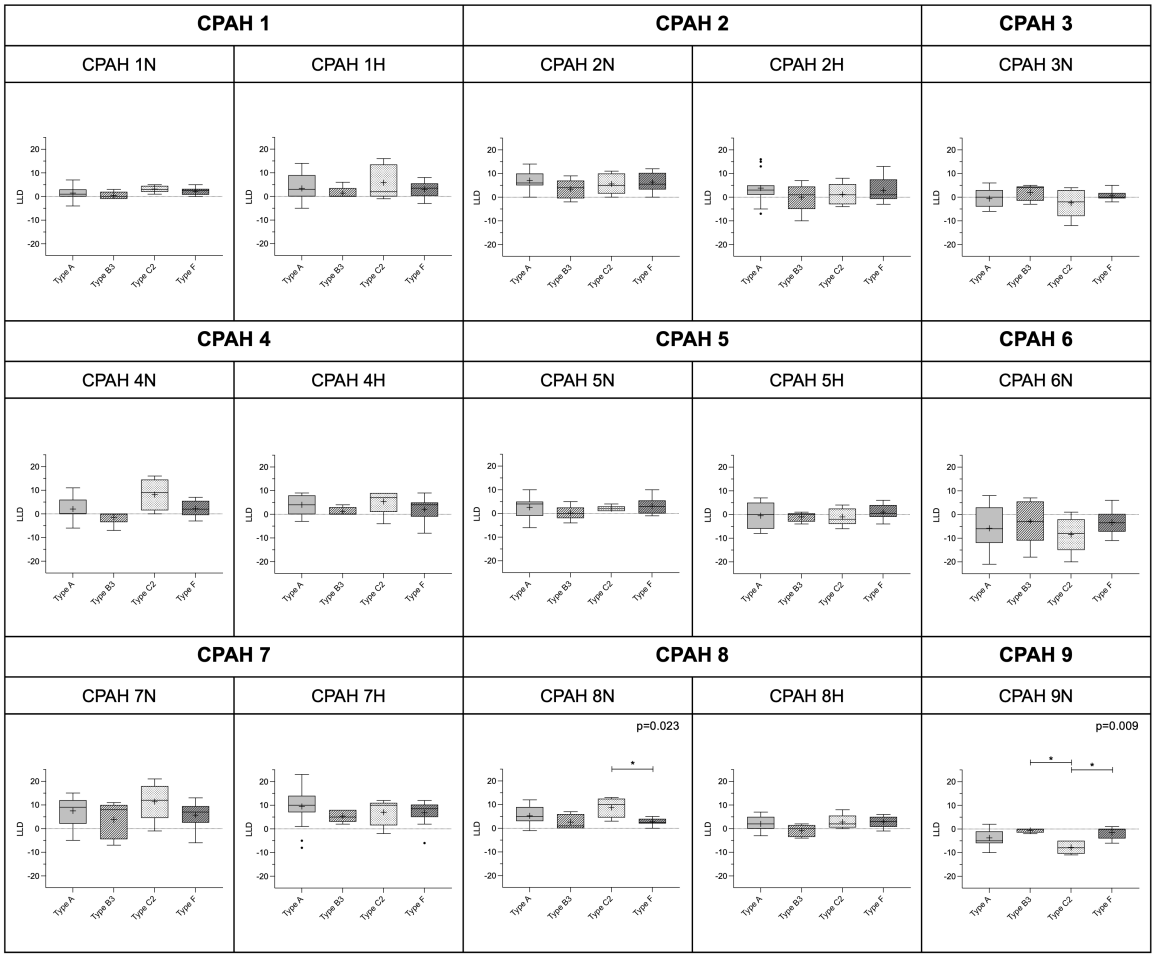
CPAH 1
CPAH 1N
CPAH 1H
CPAH 2
CPAH 2N
CPAH 2H
CPAH 3
CPAH 3N
CPAH 4
CPAH 4N
CPAH 4H
CPAH 5
CPAH 5N
CPAH 5H
CPAH 6
CPAH 6N
CPAH 7
CPAH 7N
CPAH 7H
CPAH 8
CPAH 8N
p=0.023
CPAH 8H
CPAH 9
CPAH 9N
p=0.009
LLD
Type A
Type B3
Type C2
Type F

B

Figure 5: The boxplots demonstrate the results of digital templating for (A) FO reconstruction, and (B) LLD for each stem design in the distinct CPAH types.

Plus symbols represent mean values, and lines mark the median values. Asterisks denote statistical significance, *$P < 0.05$, **$P < 0.010$, ***$P < 0.001$.

ΔFO, femoral offset reconstruction (planned – preoperative); LLD, leg-length discrepancy (affected minus contralateral hip).

Tables

Table 1 Distribution and percentages of CPAH types.

	Coxa vara (NSA < 120°)		**Coxa norma** (NSA 120 – 140°)		**Coxa valga** (NSA > 140°)	
	FOR_N	FOR_H	FOR_N	FOR_H	FOR_N	FOR_H
Dorr A (CI > 0.6)	40 (1.71%)	39 (1.66%)	517 (22.05%)	91 (3.88%)	47 (2.00%)	0 (0.00%)
Dorr B (CI 0.6-0.5)	40 (1.71%)	51 (2.17%)	897 (38.25%)	149 (6.35%)	158 (6.74%)	0 (0.00%)
Dorr C (CI < 0.5)	9 (0.38%)	12 (0.51%)	207 (8.83%)	29 (1.24%)	59 (2.52%)	0 (0.00%)

CI, cortical index; FOR, femoral offset ratio; NSA, neck-shaft angle.

Table 2 Demographic characteristics and geometric parameters of proximal femoral anatomy in CPAH types.

	CPAH 1N (n=40)		**CPAH 1H** (n=39)		**CPAH 2N** (n=517)		**CPAH 2H** (n=91)		**CPAH 3N** (n=47)		**P-value**
Age, mean (SD)	67.8	(13.2)	69.1	(11.2)	63.7	(11.0)	67.7	(8.9)	59.3	(11.1)	
Sex											
women, %	17	(42.5)	17	(43.6)	274	(53.0)	59	(64.8)	37	(78.7)	
men, %	23	(57.5)	22	(56.4)	243	(47.0)	32	(35.2)	10	(21.3)	
BMI, mean (SD)	29.8	(4.1)	27.4	(4.9)	29.7	(5.5)	26.9	(3.7)	30.5	(4.4)	
CI, mean (SD)	0.64	(0.0)	0.6	(0.0)	0.6	(0.0)	0.6	(0.0)	0.6	(0.0)	
NSA, mean (SD)	116.9	(2.9)	117.1	(2.4)	129.9	(4.9)	125.4	(3.6)	144.3	(3.9)	
FO, mean (SD)	55.0	(8.1)	59.6	(4.9)	46.8	(6.2)	54.8	(5.6)	33.1	(6.0)	
FOR, mean (SD)	1.5	(0.1)	1.7	(0.1)	1.4	(0.1)	1.7	(0.1)	1.1	(0.2)	

	CPAH 4N (n=40)		**CPAH 4H** (n=51)		**CPAH 5N** (n=897)		**CPAH 5H** (n=149)		**CPAH 6N** (n=158)		
Age, mean (SD)	70.8	(11.0)	69.5	(11.0)	66.7	(11.5)	69.8	(9.8)	62.7	(11.4)	
Sex											
women, %	19	(47.5)	28	(54.9)	504	(56.2)	112	(75.2)	121	(76.6)	
men, %	21	(52.5)	23	(45.1)	393	(43.8)	37	(24.8)	37	(23.4)	
BMI, mean (SD)	27.5	(4.93)	26.5	(3.8)	27.7	(5.3)	25.4	(4.0)	27.6	(5.2)	
CI, mean (SD)	0.6	(0.0)	0.6	(0.0)	0.6	(0.0)	0.6	(0.0)	0.6	(0.0)	
NSA, mean (SD)	117.1	(2.8)	115.7	(3.9)	130.5	(4.9)	126.2	(3.8)	143.7	(3.6)	
FO, mean (SD)	52.3	(4.5)	58.4	(6.2)	45.8	(6.1)	53.0	(4.8)	34.0	(5.2)	
FOR, mean (SD)	1.5	(0.1)	1.7	(0.1)	1.4	(0.1)	1.7	(0.1)	1.1	(0.2)	

	CPAH 7N (n=9)		**CPAH 7H** (n=12)		**CPAH 8N** (n=207)		**CPAH 8H** (n=29)		**CPAH 9N** (n=59)		
Age, mean (SD)	67.9	(12.4)	70.8	(12.1)	69.3	(10.6)	71.5	(13.1)	65.4	(10.7)	**<0.001 ***
Sex											**<0.001 ***
women, %	6	(66.7)	10	(83.3)	142	(68.6)	19	(65.5)	46	(78.0)	
men, %	3	(33.3)	2	(16.7)	65	(31.4)	10	(34.5)	13	(22.0)	
BMI, mean (SD)	24.9	(4.4)	23.4	(3.2)	26.3	(6.0)	24.8	(4.9)	25.9	(5.4)	**<0.001 ***
CI, mean (SD)	0.5	(0.0)	0.5	(0.0)	0.5	(0.0)	0.5	(0.1)	0.5	(0.0)	**<0.001 ***
NSA, mean (SD)	117.5	(3.2)	116.2	(2.8)	131.1	(5.4)	125.9	(3.7)	145.0	(4.0)	**<0.001 ***
FO, mean (SD)	48.8	(6.9)	57.5	(7.2)	44.8	(6.2)	53.8	(4.7)	33.3	(5.4)	**<0.001 ***
FOR, mean (SD)	1.4	(0.1)	1.7	(0.1)	1.4	(0.1)	1.8	(0.2)	1.1	(0.2)	**<0.001 ***

BMI, body mass index; CI, cortical index; FO, femoral offset; FOR, femoral offset ratio; NSA, neck shaft angle, SD, standard deviation.
Asterisks indicate statistical significance (P < 0.05); Kruskal-Wallis Test with Bonferroni adjustment for multiple testing.

Table 3 Digital templating results stratified by CPAH types and stem design.

Reconstructive parameter	Stem design								
CPAH 1N	Straight Stem (Type A)		Quadrangular Taper Stem (Type B3)		Anatomic Stem (Type C2)		Short Stem (Type F)		P-value
ΔFO, mean (SD), range	-2.1 (2.9)	-7.0 - 3.0	1.6 (1.1)	0.0 - 3.0	-0.2 (5.7)	-6.0 - 7.0	2.8 (1.6)	1.0 - 5.0	**0.003** * *A - F, P = 0.002*
LLD, mean (SD), range	1.5 (2.6)	-4.0 - 7.0	0.4 (1.7)	-1.0 - 3.0	3.2 (1.5)	1.0 - 5.0	2.2 (1.7)	0.0 - 5.0	0.101
Adequate THA reconstruction, n (%)	5 (33.3)		5 (100.0)		1 (20.0)		10 (100.0)		**< 0.001** *
Offset restoration, n (%)	6 (40.0)		5 (100.0)		2 (40.0)		10 (100.0)		**0.003** *
Acceptable LLD, n (%)	15 (100.0)		5 (100.0)		5 (100.0)		10 (100.0)		n.a.
Agreement anatomy - stem design, n (%)	12 (80.0)		5 (100.0)		3 (60.0)		10 (100.0)		0.133

Reconstructive parameter	Stem design								
CPAH 1H	Straight Stem (Type A)		Quadrangular Taper Stem (Type B3)		Anatomic Stem (Type C2)		Short Stem (Type F)		P-value
ΔFO, mean (SD), range	-4.8 (4.6)	-13.0 - 2.0	0.4 (2.2)	-3.0 - 3.0	-1.8 (3.3)	-7.0 - 2.0	1.4 (1.5)	0.0 - 4.0	**0.002** * *A - F, p = 0.002*
LLD, mean (SD), range	3.4 (5.7)	-5.0 - 14.0	1.4 (2.6)	0.0 - 6.0	5.8 (7.3)	-1.0 - 16.0	3.0 (3.5)	-3.0 - 8.0	0.591
Adequate THA reconstruction, n (%)	2 (13.3)		3 (60.0)		2 (40.0)		10 (100.0)		**< 0.001** *
Offset restoration, n (%)	3 (20.0)		4 (80.0)		2 (40.0)		10 (100.0)		**< 0.001** *
Acceptable LLD, n (%)	13 (86.7)		5 (100.0)		3 (60.0)		10 (100.0)		0.111
Agreement anatomy - stem design, n (%)	9 (60.0)		3 (60.0)		4 (80.0)		10 (100.0)		0.128

CPAH 2N	Straight Stem (Type A)		Quadrangular Taper Stem (Type B3)		Anatomic Stem (Type C2)		Short Stem (Type F)		P-value
ΔFO, mean (SD), range	1.0 (3.1)	-9.0 - 5.0	2.6 (1.8)	1.0 - 5.0	0.0 (3.8)	-4.0 - 4.0	2.4 (1.7)	0.0 - 5.0	0.428
LLD, mean (SD), range	1.6 (8.1)	-14.0 - 11.0	-1.2 (3.7)	-6.0 - 3.0	0.2 (7.6)	-10.0 - 8.0	1.4 (5.6)	-7.0 - 9.0	0.868
Adequate THA reconstruction, n (%)	8 (55.3)		2 (40.0)		3 (60.0)		9 (90.0)		0.181
Offset restoration, n (%)	14 (93.3)		5 (100.0)		3 (60.0)		10 (100.0)		0.051
Acceptable LLD, n (%)	11 (73.3)		4 (80.0)		4 (80.0)		9 (90.0)		0.791
Agreement anatomy - stem design, n (%)	12 (80.0)		4 (80.0)		4 (80.0)		10 (100.0)		0.506

CPAH 2H	Straight Stem (Type A)		Quadrangular Taper Stem (Type B3)		Anatomic Stem (Type C2)		Short Stem (Type F)		P-value
ΔFO, mean (SD), range	-1.6 (3.4)	-7.0 - 4.0	1.2 (0.8)	0.0 - 2.0	-1.8 (3.5)	-5.0 - 2.0	1.0 (1.4)	0.0 - 4.0	0.205
LLD, mean (SD), range	3.9 (6.5)	-7.0 - 16.0	0.0 (6.2)	-10.0 - 7.0	1.2 (4.7)	-4.0 - 8.0	2.9 (5.3)	-3.0 - 13.0	0.589
Adequate THA reconstruction, n (%)	4 (26.7)		3 (60.0)		2 (40.0)		9 (90.0)		**0.018** *
Offset restoration, n (%)	6 (40.0)		5 (100.0)		2 (40.0)		10 (100.0)		**0.003** *
Acceptable LLD, n (%)	11 (73.3)		4 (80.0)		5 (100.0)		9 (90.0)		0.497
Agreement anatomy - stem design, n (%)	11 (73.3)		5 (100.0)		5 (100.0)		10 (100.0)		0.111

CPAH 3N	Straight Stem (Type A)		Quadrangular Taper Stem (Type B3)		Anatomic Stem (Type C2)		Short Stem (Type F)		P-value
ΔFO, mean (SD), range	7.7 (1.8)	5.0 - 10.0	7.0 (1.0)	6.0 - 8.0	15.2 (1.6)	13.0 - 17.0	5.7 (1.9)	3.0 - 9.0	**< 0.001** * *F - C2, P < 0.001* *B3 - C2, P = 0.038* *A - C2, P = 0.043*
LLD, mean (SD), range	-0.6 (4.0)	-6.0 - 6.0	2.0 (3.4)	-3.0 - 5.0	-2.4 (6.2)	-12.0 - 4.0	0.6 (2.3)	-2.0 - 5.0	0.306
Adequate THA reconstruction, n (%)	1 (6.7)		0 (0.0)		0 (0.0)		1 (10.0)		0.808
Offset restoration, n (%)	3 (20.0)		0 (0.0)		0 (0.0)		5 (50.0)		0.065
Acceptable LLD, n (%)	14 (93.3)		5 (100.0)		4 (80.0)		10 (100.0)		0.419
Agreement anatomy - stem design, n (%)	4 (26.7)		4 (80.0)		2 (40.0)		8 (80.0)		**0.031** *

Reconstructive parameter	Stem design								
CPAH 4N	Straight Stem (Type A)		Quadrangular Taper Stem (Type B3)		Anatomic Stem (Type C2)		Short Stem (Type F)		P-value
ΔFO, mean (SD), range	-1.9 (3.0)	-6.0 - 3.0	1.0 (1.7)	0.0 - 4.0	-0.2 (3.7)	-5.0 - 4.0	2.4 (3.7)	0.0 - 12.0	**0.029** * *A - F, P = 0.024*
LLD, mean (SD), range	2.1 (4.8)	-6.0 - 11.0	-1.4 (3.1)	-7.0 - 0.0	8.2 (6.7)	0.0 - 16.0	2.2 (3.6)	-3.0 - 7.0	0.070
Adequate THA reconstruction, n (%)	4 (26.7)		3 (60.0)		2 (40.0)		8 (80.0)		0.065
Offset restoration, n (%)	6 (40.0)		5 (100.0)		2 (40.0)		9 (90.0)		**0.014** *
Acceptable LLD, n (%)	13 (86.7)		4 (80.0)		3 (60.0)		10 (100.0)		0.211
Agreement anatomy - stem design, n (%)	12 (80.0)		4 (80.0)		4 (80.0)		10 (100.0)		0.506

Reconstructive parameter	Stem design								
CPAH 4H	Straight Stem (Type A)		Quadrangular Taper Stem (Type B3)		Anatomic Stem (Type C2)		Short Stem (Type F)		P-value
ΔFO, mean (SD), range	-1.4 (3.2)	-9.0 - 1.0	0.6 (0.9)	0.0 - 2.0	1.6 (3.8)	-4.0 - 6.0	1.1 (1.4)	0.0 - 4.0	0.122
LLD, mean (SD), range	4 (4.1)	-3.0 - 9.0	1.2 (1.8)	0.0 - 4.0	5.4 (5.4)	-4.0 - 9.0	2.1 (5.0)	-8.0 - 9.0	0.346
Adequate THA reconstruction, n (%)	6 (40.0)		5 (100.0)		2 (40.0)		9 (90.0)		**0.014** *
Offset restoration, n (%)	8 (53.3)		5 (100.0)		3 (60.0)		10 (100.0)		**0.027** *
Acceptable LLD, n (%)	15 (100.0)		5 (100.0)		5 (100.0)		9 (90.0)		0.462
Agreement anatomy - stem design, n (%)	14 (93.3)		5 (100.0)		4 (80.0)		10 (100.0)		0.419

CPAH 5N	Straight Stem (Type A)		Quadrangular Taper Stem (Type B3)		Anatomic Stem (Type C2)		Short Stem (Type F)		P-value
ΔFO, mean (SD), range	1.8 (1.9)	-1.0 - 5.0	3.4 (2.5)	-0.0 - 7.0	6.0 (3.2)	1.0 - 10.0	2.4 (1.7)	0.0 - 5.0	**0.007** * *A - C2, P = 0.004* *F - C2, P = 0.030*
LLD, mean (SD), range	2.6 (4.1)	-6.0 - 10.0	0.2 (3.2)	-4.0 - 5.0	2.0 (1.2)	1.0 - 4.0	3.1 (3.6)	-1.0 - 10.0	0.515
Adequate THA reconstruction, n (%)	13 (86.7)		4 (80.0)		3 (60.0)		10 (100.0)		0.211
Offset restoration, n (%)	14 (93.3)		4 (80.0)		1 (20.0)		10 (100.0)		**<0.001** *
Acceptable LLD, n (%)	14 (93.3)		5 (100.0)		5 (100.0)		10 (100.0)		0.712
Agreement anatomy - stem design, n (%)	14 (93.3)		5 (100.0)		4 (80.0)		10 (100.0)		0.419

CPAH 5H	Straight Stem (Type A)		Quadrangular Taper Stem (Type B3)		Anatomic Stem (Type C2)		Short Stem (Type F)		P-value
ΔFO, mean (SD), range	1.3 (1.7)	-2.0 - 4.0	1.4 (0.9)	0.0 - 2.0	3.8 (1.9)	2.0 - 7.0	2.3 (2.0)	0.0 - 5.0	0.106
LLD, mean (SD), range	-0.5 (5.8)	-8.0 - 7.0	-1.0 (2.0)	-4.0 - 1.0	-1.0 (3.7)	-6.0 - 4.0	1.0 (3.3)	-4.0 - 6.0	0.786
Adequate THA reconstruction, n (%)	8 (53.3)		5 (100.0)		3 (60.0)		10 (100.0)		**0.027** *
Offset restoration, n (%)	13 (86.7)		5 (100.0)		4 (80.0)		10 (100.0)		0.445
Acceptable LLD, n (%)	10 (66.7)		5 (100.0)		4 (80.0)		10 (100.0)		0.117
Agreement anatomy - stem design, n (%)	15 (100.0)		5 (100.0)		5 (100.0)		10 (100.0)		n.a.

CPAH 6N	Straight Stem (Type A)		Quadrangular Taper Stem (Type B3)		Anatomic Stem (Type C2)		Short Stem (Type F)		P-value
ΔFO, mean (SD), range	5.5 (1.6)	3.0 - 9.0	2.3 (1.3)	2.0 - 5.0	11.0 (3.2)	7.0 - 15.0	2.9 (1.7)	1.0 - 6.0	**< 0.001** * *F - A, P = 0.032* *F - C2, P < 0.001* *B3 - C2, P < 0.005*
LLD, mean (SD), range	-5.8 (8.6)	-21.0 - 8.0	-2.8 (9.7)	-18.0 - 7.0	-8.4 (7.7)	-20.0 - 1.0	-3.3 (5.0)	-11.0 - 6.0	0.578
Adequate THA reconstruction, n (%)	2 (13.3)		4 (80.0)		0 (0.0)		4 (40.0)		**0.013** *
Offset restoration, n (%)	7 (46.7)		5 (100.0)		0 (0.0)		9 (90.0)		**0.001** *
Acceptable LLD, n (%)	6 (40.0)		4 (80.0)		2 (40.0)		6 (60.0)		0.396
Agreement anatomy - stem design, n (%)	8 (53.3)		5 (100.0)		1 (20.0)		6 (60.0)		0.083

Reconstructive parameter	Stem design								
CPAH 7N	Straight Stem (Type A)		Quadrangular Taper Stem (Type B3)		Anatomic Stem (Type C2)		Short Stem (Type F)		P-value
ΔFO, mean (SD), range	-0.9 (2.2)	-6.0 - 2.0	2.4 (2.1)	0.0 - 5.0	8.0 (3.8)	4.0 - 14.0	0.8 (0.6)	0.0 - 2.0	**< 0.001 *** *A - C2, P < 0.001*
LLD, mean (SD), range	7.5 (6.5)	-5.0 - 15.0	3.8 (7.9)	-7.0 - 11.0	11.4 (8.1)	-1.0 - 21.0	5.7 (5.8)	-6.0 - 13.0	0.208
Adequate THA reconstruction, n (%)	3 (20.0)		3 (60.0)		0 (0.0)		7 (70.0)		**0.014 ***
Offset restoration, n (%)	8 (53.3)		5 (100.0)		1 (20.0)		10 (100.0)		**0.003 ***
Acceptable LLD, n (%)	9 (60.0)		3 (60.0)		2 (40.0)		7 (70.0)		0.741
Agreement anatomy - stem design, n (%)	13 (86.7)		5 (100.0)		0 (0.0)		10 (100.0)		**< 0.001 ***

Reconstructive parameter	Stem design								
CPAH 7H	Straight Stem (Type A)		Quadrangular Taper Stem (Type B3)		Anatomic Stem (Type C2)		Short Stem (Type F)		P-value
ΔFO, mean (SD), range	-3,0 (4,0)	-10.0 - 3.0	0.2 (2.2)	-3.0 - 3.0	3.6 (3.8)	0.0 - 10.0	0.5 (0.8)	0.0 - 2.0	**0.007 *** *A - C2, P = 0.006*
LLD, mean (SD), range	9.5 (8.4)	-8.0 - 23.0	5.4 (2.6)	2.0 - 8.0	7.0 (5.7)	-2.0 - 12.0	6.8 (5.3)	-6.0 - 12.0	0.609
Adequate THA reconstruction, n (%)	1 (6.7)		3 (60.0)		2 (40.0)		7 (70.0)		**0.008 ***
Offset restoration, n (%)	5 (33.3)		4 (80.0)		4 (80.0)		10 (100.0)		**0.004 ***
Acceptable LLD, n (%)	7 (46.7)		5 (100.0)		4 (80.0)		7 (70.0)		0.135
Agreement anatomy - stem design, n (%)	7 (46.7)		3 (60.0)		3 (60.0)		9 (90.0)		0.181

CPAH 8N	Straight Stem (Type A)		Quadrangular Taper Stem (Type B3)		Anatomic Stem (Type C2)		Short Stem (Type F)		P-value
ΔFO, mean (SD), range	1.2 (1.5)	0.0 - 4.0	1.0 (0.7)	0.0 - 2.0	10.2 (2.6)	7.0 - 13.0	0.8 (0.8)	0.0 - 2.0	**0.004 *** *F - C2, P = 0.004* *A - C2, P = 0.004*
LLD, mean (SD), range	5.3 (3.7)	-1.0 - 12.0	2.6 (3.2)	0.0 - 7.0	8.8 (4.2)	3.0 - 13.0	2.8 (1.5)	0.0 - 5.0	**0.023 *** *F - C2, P = 0.004*
Adequate THA reconstruction, n (%)	10 (66.7)		5 (100.0)		0 (0.0)		10 (100.0)		**< 0.001 ***
Offset restoration, n (%)	15 (100.0)		5 (100.0)		0 (0.0)		10 (100.0)		**< 0.001 ***
Acceptable LLD, n (%)	13 (86.7)		5 (100.0)		3 (60.0)		10 (100.0)		0.111
Agreement anatomy - stem design, n (%)	12 (80.0)		5 (100.0)		1 (20.0)		10 (100.0)		**0.002 ***

CPAH 8H	Straight Stem (Type A)		Quadrangular Taper Stem (Type B3)		Anatomic Stem (Type C2)		Short Stem (Type F)		P-value
ΔFO, mean (SD), range	0.4 (1.6)	-4.0 - 2.0	1.6 (0.9)	1.0 - 3.0	3.2 (3.3)	0.0 - 8.0	1.2 (1.6)	0.0 - 5.0	0.196
LLD, mean (SD), range	2 (2.9)	-3.0 - 7.0	-0.8 (2.6)	-4.0 - 2.0	2.8 (3.1)	0.0 - 8.0	2.9 (2.4)	-1.0 - 6.0	0.164
Adequate THA reconstruction, n (%)	10 (66.7)		5 (100.0)		3 (60.0)		10 (100.0)		0.083
Offset restoration, n (%)	13 (66.7)		5 (100.0)		4 (80.0)		10 (100.0)		0.445
Acceptable LLD, n (%)	15 (100.0)		5 (100.0)		5 (100.0)		10 (100.0)		n.a.
Agreement anatomy - stem design, n (%)	12 (80.0)		5 (100.0)		3 (60.0)		10 (100.0)		0.133

CPAH 9N	Straight Stem (Type A)		Quadrangular Taper Stem (Type B3)		Anatomic Stem (Type C2)		Short Stem (Type F)		P-value
ΔFO, mean (SD), range	7.1 (3.2)	0.0 - 13.0	6.6 (2.2)	4.0 - 10.0	13.2 (0.8)	12.0 - 14.0	5.9 (2.7)	3.0 - 10.0	**< 0.001 *** *C2 - A, P < 0.001* *C2 - B3, P = 0.004* *C2 - F, P < 0.001*
LLD, mean (SD), range	-3.7 (3.5)	-10.0 - 2.0	-0.6 (0.9)	-2.0 - 0.0	-7.8 (2.8)	-11.0 - -5.0	-1.5 (2.4)	-6.0 - 1.0	**0.009 *** *C2 - F, P = 0.018* *C2 - B3, P = 0.024*
Adequate THA reconstruction, n (%)	4 (26.7)		1 (20.0)		0 (0.0)		2 (20.0)		0.644
Offset restoration, n (%)	5 (33.3)		1 (20.0)		0 (0.0)		5 (50.0)		0.239
Acceptable LLD, n (%)	10 (66.7)		5 (100.0)		2 (40.0)		9 (90.0)		0.087
Agreement anatomy - stem design, n (%)	7 (46.7)		5 (100.0)		2 (40.0)		10 (100.0)		**0.007 ***

Type A, Flat Taper Stem (Stryker ® Accolade, Zimmer Biomet ® Taperloc, BBraun Aesculap ® Bicontact); Type B3, Quadrangular Taper Stem (BBraun Aesculap ® CoreHip), Type C2, Anatomic Fit-and-Fill Stem (Symbios ® SPS stem), Type F, Short Stem (Mathys ® Optimys, Artiqo ® A2) .

FO, femoral offset; FOR, femoral offset ratio; NSA, neck shaft angle; SD, standard deviation.

Asterisks indicate statistical significance (P<0.05); Kruskal-Wallis Test with Bonferroni adjustment for multiple testing, Chi-square test

Supplemental Table S1A Digital templating results for FO reconstruction stratified by CPAH types and stem design.

	Straight Stem (Type A)			**Quadrangular Taper Stem (Type B3)**			**Anatomic Stem (Type C2)**			**Short Stem (Type F)**			**p-value**
	ΔFO, mean (SD)		range	ΔFO, mean (SD)		range	ΔFO, mean (SD)		range	ΔFO, mean (SD)		range	
NSA subgroups													
Coxa vara (n=210)	-2.4	(3.6)	-13.0 - 3.0	1.0	(1.8)	-3.0 - 5.0	1.8	(5.0)	-7.0 - 14.0	1.5	(2.0)	0.0 - 12.0	**<0.001 *** *A – B3, p<0.001* *A – C2, p<0.001* *A – F, p<0.001*
Coxa norma (n=210)	0.7	(2.5)	-9.0 - 5.0	1.9	(1.6)	0.0 - 7.0	3.6	(4.9)	-5.0 - 13.0	1.7	(1.7)	0.0 - 5.0	**<0.001 *** *A – C2, p=0.001*
Coxa valga (n=105)	6.8	(2.5)	0.0 - 13.0	5.6	(2.3)	2.0 - 10.0	13.1	(2.6)	7.0 - 17.0	4.8	(2.5)	1.0 - 10.0	**<0.001 *** *F – A, p=0.032* *F – C2, p<0.001* *B3 – C2, p<0.001* *A – C2, p<0.001*
Dorr types													
Dorr A (n=175)	0.0	(5.3)	-13.0 - 10.0	2.6	(2.7)	-3.0 - 8.0	2.3	(7.5)	-7.0 - 17.0	2.7	(2.3)	0.0 - 9.0	**0.007 *** *A – F, p=0.009*
Dorr B (n=175)	1.1	(3.5)	-9.0 - 9.0	1.9	(1.9)	0.0 - 7.0	4.4	(5.0)	-5.0 - 15.0	2.2	(2.2)	0.0 - 12.0	**0.006 *** *A – C2, p=0.003*
Dorr C (n=175)	1.0	(4.3)	-10.0 - 13.0	2.4	(2.8)	-3.0 - 10.0	7.6	(4.8)	0.0 - 14.0	1.8	(2.5)	0.0 - 10.0	**<0.001 *** *A – C2, p<0.001* *F – C2, p<0.001*
FOR subgroups													
FOR_N (n=315)	2.1	(4.3)	-9.0 - 13.0	3.2	(2.6)	0.0 - 10.0	7.0	(6.5)	-6.0 - 17.0	2.9	(2.6)	0.0 - 12.0	**<0.001 *** *A – C2, p<0.001* *F – C2, p<0.001* *B3 – C2, p=0.018*
FOR_H (n=210)	-1.5	(3.8)	-13.0 - 4.0	0.9	(1.4)	-3.0 - 3.0	1.4	(3.9)	-7.0 - 10.0	1.25	(1.6)	0.0 - 5.0	**<0.001 *** *A – F, p<0.001* *A – B3, p=0.011* *A – C2, p=0.001*

FO, femoral offset; FOR, femoral offset ratio; NSA, neck shaft angle, SD, standard deviation.
Asterisks indicate statistical significance (P<0.05); Kruskal-Wallis Test with Bonferroni adjustment for multiple testing.

Supplemental Table S1B Digital templating results for leg length reconstruction stratified by CPAH types and stem design

	Straight Stem (Type A)			**Quadrangular Taper Stem (Type B3)**			**Anatomic Stem (Type C2)**			**Short Stem (Type F)**			**p-value**
	LLD, mean (SD)		range	LLD, mean (SD)		range	LLD, mean (SD)		range	LLD, mean (SD)		range	
NSA subgroups													
Coxa vara (n=210)	4.6	(6.2)	-8.0 - 23.0	1.8	(4.2)	-7.0 - 11.0	6.8	(6.2)	-4.0 - 21.0	3.7	(4.6)	-8.0 - 13.0	**0.007 *** *B3 – C2, p=0.004*
Coxa norma (n=210)	2.5	(5.6)	-14.0 - 16.0	0.0	(3.6)	-10.0 - 7.0	2.3	(5.2)	-10.0 - 13.0	2.4	(3.8)	-7.0 - 13.0	**0.019 *** *B3 – F, p=0.011*
Coxa valga (n=105)	-3.4	(6.1)	-21.0 - 8.0	-0.5	(5.9)	-18.0 - 7.0	-6.2	(6.2)	-20.0 - 4.0	-1.4	(3.7)	-11.0 - 6.0	**0.013 *** *C2 – B3, p=0.019*
Dorr types													
Dorr A (n=175)	1.9	(5.8)	-14.0 - 16.0	0.5	(3.7)	-10.0 - 7.0	1.6	(6.1)	-12.0 - 16.0	2.0	(4.0)	-7.0 - 13.0	0.537
Dorr B (n=175)	0.5	(6.6)	-21.0 - 11.0	-0.8	(4.7)	-18.0 - 7.0	1.2	(7.7)	-20.0 - 16.0	1.0	(4.6)	-11.0 - 10.0	0.385
Dorr C (n=175)	4.1	(7.1)	-10.0 - 23.0	2.1	(4.5)	-7.0 - 11.0	4.4	(8.3)	-11.0 - 21.0	3.3	(4.7)	-6.0 - 13.0	0.392
FOR subgroups													
FOR_N (n=315)	1.1	(6.6)	-21.0 - 15.0	0.3	(4.9)	-18.0 - 11.0	1.7	(8.5)	-20.0 - 21.0	1.5	(4.4)	-11.0 - 13.0	0.494
FOR_H (n=210)	3.7	(6.4)	-8.0 - 23.0	1.0	(3.7)	-10.0 - 8.0	3.5	(5.5)	-6.0 - 16.0	3.1	(4.5)	-8.0 - 13.0	0.111

FOR, femoral offset ratio; LLD, leg length difference; NSA, neck shaft angle, SD, standard deviation.
Asterisks indicate statistical significance (P<0.05); Kruskal-Wallis Test with Bonferroni adjustment for multiple testing.